Available online at www.sciencedirect.com
ScienceDirect
Materials Science and Engineering C 28 (2008) 129–140
MATERIALS SCIENCE & ENGINEERING C
www.elsevier.com/locate/msec

Using a synthetic body fluid (SBF) solution of 27 mM HCO_3^- to make bone substitutes more osteointegrative ☆

Sahil Jalota [a], Sarit B. Bhaduri [a], A. Cuneyt Tas [b,*]

[a] *School of Materials Science and Engineering, Clemson University, Clemson, SC 29634, USA*
[b] *Department of Biomedical Engineering, Yeditepe University, Istanbul 34755, Turkey*

Received 13 August 2007; received in revised form 2 October 2007; accepted 10 October 2007
Available online 17 October 2007

Abstract

A Tris–HCl-buffered synthetic body fluid (SBF) solution, mimicking the human blood plasma, with the following ion concentrations of 27 mM HCO_3^-, 2.5 mM Ca^{2+}, 1.0 mM HPO_4^{2-}, 142 mM Na^+, 125 mM Cl^-, 5 mM K^+, 1.5 mM Mg^{2+}, and 0.5 mM SO_4^{2-} was used as an aqueous medium to process a number of bone substitute materials under the so-called biomimetic conditions of 37 °C and pH 7.4. This solution was named as Tris–SBF-27 mM. Firstly, collagen sponges were soaked in Tris–SBF-27 mM solution at 37 °C and were found to be fully covered with nanoporous apatitic calcium phosphate (Ap-CaP). The composites of collagen–Ap-CaP biomaterials are expected to be used in orthopedic and dental surgery. Secondly, Ap-CaP short whiskers or microrods with a novel nanotexture and surface areas higher than 45 m^2/g were synthesized in Tris–SBF-27 mM solution. Thirdly, calcium sulfate cements doped with $CaHPO_4$ (monetite), were shown to have apatite-inducing ability upon ageing in Tris–SBF-27 mM. $CaHPO_4$ addition in calcium sulfate was found to improve its mechanical strength, measured after cement setting reaction. Pure calcium sulfate cement pellets were not stable in Tris–SBF-27 mM solutions and crumbled into a powder. All the samples were characterized by SEM, XRD, FTIR, surface area and mechanical strength measurements.

Keywords: Bone substitute; Calcium phosphate; Biomaterial; Synthesis; Body fluid; Biomimetic

1. Introduction

The historical development of synthetic or simulated body fluids (SBF, which claim to mimic the acellular human blood plasma) cannot be pictured accurately without mentioning the Ringer's solution of 1880 [1], Earle's balanced salt solution (*EBSS*) of 1943 [2] and Hanks' balanced salt solution (*HBSS*) of 1949 [3]. SBF solutions developed by T. Kokubo between 1990 [4] and 2006 [5] may be considered as close relatives of EBSS and HBSS.

The ion concentrations of acellular human blood plasma and some physiological solutions are compared in Table 1. HBSS and EBSS solutions, on the other hand, are commercially available today as either supplemented with glucose or with amino acids and vitamins, and are commonly used in tissue engineering or cell culture studies. Solutions such as HBSS and EBSS do help to maintain intra- and extracellular osmotic balance, provide cells with water and certain bulk inorganic ions essential for normal cell metabolism, and provide a buffering system to maintain the medium within the physiological pH range (7.2–7.6) [6].

The HCO_3^- concentration of the EBSS solution (i.e., 26.2 mM) resembles that of human plasma (27 mM). On the other hand, the carbonate ion concentration of the HBSS solution is much lower than that (i.e., 4.2 mM). The SBF (*simulated body fluid*) solution resembled to a Tris–HCl-buffered (at pH 7.4 and 37 °C) HBSS solution whose Ca/P molar ratio was adjusted to 2.50, and whose Mg^{2+} concentration was increased from 0.81 (HBSS) to 1.5 mM [4]. The original HBSS solution had a Ca/P molar ratio of 1.62, whereas the same ratio in EBSS was 1.80 [7,8].

☆ Notes: Certain commercial equipment, instruments or materials are identified in this paper to foster understanding. Such identification does not imply recommendation or endorsement by the author, nor does it imply that the equipment or materials identified are necessarily the best available for the purpose.

* Corresponding author. Tel.: +90 216 5780000x3361; fax: +90 216 5780400.
E-mail address: actas@yeditepe.edu.tr (A.C. Tas).

0928-4931/$ - see front matter © 2007 Elsevier B.V. All rights reserved.
doi:10.1016/j.msec.2007.10.058

Table 1
Ion concentrations of human plasma and synthetic solutions, mM

	Human plasma	Ringer [1]	EBSS [2]	HBSS [3]	*Kokubo*–SBF [4]	*Tas*–SBF [13,14]
Na^+	142	130	143.6	138	142	142
K^+	5	4	5.37	6.14	5	5
Ca^{2+}	2.5	1.4	1.8	1.26	2.5	2.5
Mg^{2+}	1.5		0.81	0.81	1.5	1.5
Cl^-	103	109	125.3	144.8	147.8	125
HCO_3^-	27		26.2	4.2	4.2	27
HPO_4^{2-}	1		1	0.78	1	1
SO_4^{2-}	0.5		0.81	0.81	0.5	0.5
Ca/P	2.5		1.8	1.62	2.5	2.5
Buffer					*Tris*	*Tris*
pH	7.4	6.5	7.2–7.6	6.7–6.9	7.4	7.4

Is it possible to convert an HBSS solution of 4.2 mM HCO_3^- into an SBF of 4.2 mM HCO_3^-? As shown in Table 1, HBSS has an HPO_4^{2-} concentration of 0.78 mM, and in order to raise this value to 1 mM, one simply needs to add 31.2 mg of anhydrous Na_2HPO_4 to 1 L of a commercially available HBSS solution. By this addition of Na_2HPO_4, the Na^+ concentration of the HBSS solution would increase to 138.44 (from 138 mM). In order to raise the Ca/P molar ratio of the above solution to 2.50, one must add 182.3 mg of $CaCl_2{\cdot}2H_2O$ into this solution. After this addition of Ca-chloride dihydrate, the new solution will have a Ca^{2+} concentration of 2.5 mM (therefore, a Ca/P ratio of 2.50) and Cl^- concentration of 147.28 mM. A small aliquot of 1 M HCl solution can be added (before the introduction of $CaCl_2{\cdot}2H_2O$) to prevent premature CaP precipitation in the solution. Finally, in order to increase the Mg^{2+} concentration of 1 L of the above solution to 1.5 mM, one must add and dissolve 140.3 mg $MgCl_2{\cdot}6H_2O$. This addition will also raise its Cl^- concentration to 147.8 mM. All of these additions do not alter the HCO_3^- concentration, and it will remain constant at 4.2 mM. Adjusting the pH of this solution can easily be achieved by using the Tris (*tris-hydroxymethyl-aminomethane*)–HCl couple. The original SBF solution was, therefore, unable to mimic the human blood plasma in terms of one of its most important ions, namely HCO_3^- [4].

The reader is hereby advised to refer to an experimental comparison of HBSS and the above-mentioned solutions, in terms of their CaP-depositing capacities, being reported in the work of Serro and Saramago [9]. It is a well-known fact that even a pristine HBSS solution is able to deposit CaP on titanium surfaces, but at a much slower pace in comparison to SBF solutions [10–14].

Hepes (*2-(4-(2-hydroxyethyl)-1-piperazinyl)ethane sulphonic acid*), instead of Tris, was also used to stabilize the pH of SBF-like solutions at 7.4 [15]. However, Oyane et al. [15] reported, in comparison to *Tris–HCl-buffered* SBF solutions, that *Hepes–NaOH-buffered* SBF would easily release CO_2 gas from the solution, causing a decrease in its nominal HCO_3^- concentration, and an increase in its pH value, when the storage period was long. Furthermore, Oyane et al. [15] stated that Hepes–NaOH-buffered SBF would not be suitable for long-term use in the biomimetic CaP formation or deposition processes owing to its instability. On the other hand, Ogino et al. [16] have pointed out as early as 1980 that the *in vivo* calcium phosphate formation on glasses can be simulated best in a Tris–HCl-buffered synthetic solution of pH 7.4.

HBSS and EBSS solutions are manufactured on the commercial scale (for instance, by Sigma-Aldrich Corp.) by using the starting inorganic salts of NaCl, KCl, $MgSO_4$, $CaCl_2{\cdot}2H_2O$, KH_2PO_4/NaH_2PO_4 (or Na_2HPO_4) and $NaHCO_3$ [6]. Therefore, in preparing synthetic body fluids one should avoid the use of hygroscopic $CaCl_2$, which rapidly attracts moisture from the atmosphere, in stark contrast to what has always been suggested in the articles of Kokubo [4,5]. SBF solutions must instead be prepared by using $CaCl_2{\cdot}2H_2O$, similar to what the manufacturers of HBSS and EBSS do [6].

This study presents a detailed recipe for preparing Tris–HCl-buffered SBF solutions with an HCO_3^- concentration of 27 mM (just like the human plasma), and exemplifies the use of this solution in synthesizing unique bone substitute (graft) biomaterials, such as biomimetic CaP microrods, collagen–CaP composites, and monetite ($CaHPO_4$)-doped calcium sulfate composites for musculoskeletal repair applications. The Tris–SBF-27 mM solution was originally developed by one of the current authors back in 1999–2000 and used in that period to produce Na, K and Mg-doped apatitic calcium phosphate powders under the biomimetic conditions of 37 °C and pH 7.4 [13,14]. The biomimetic CaP deposition ability of Tris–SBF-27 mM solutions (in direct comparison to Kokubo–SBF solutions) on titanium and its alloys was recently reported elsewhere [17]. On the other hand, the use of the Tris–SBF-27 mM solution of this study has also been tested in improving the biocompatibility of a common polymer such as PTFE (i.e., Teflon®) by Grondahl et al. [18].

2. Experimental

2.1. Preparation of synthetic body fluid (SBF)

The following reagent-grade chemicals were used in preparing Tris–HCl-buffered SBF solutions of 27 mM HCO_3^- in deionized water [13,14]:

(1) sodium chloride (NaCl),
(2) potassium chloride (KCl),
(3) sodium hydrogen carbonate ($NaHCO_3$),
(4) magnesium chloride hexahydrate ($MgCl_2{\cdot}6H_2O$),
(5) sodium sulphate (Na_2SO_4),
(6) calcium chloride dihydrate ($CaCl_2{\cdot}2H_2O$),
(7) di-sodium hydrogen phosphate dihydrate ($Na_2HPO_4{\cdot}2H_2O$),
(8) Tris ($(CH_2OH)_3CNH_2$),
(9) 1 M HCl solution.

It is extremely important not to use KCl and $K_2HPO_4{\cdot}3H_2O$ at the same time during the preparation of Tris–HCl-buffered SBF, since this will only lead to an SBF solution with low HCO_3^- concentration (i.e., 4.2 mM). The use of di-sodium hydrogen phosphate in place of di-potassium hydrogen phosphate ensures the attainment of 27 mM HCO_3^- in a Tris–HCl-buffered SBF solution.

Table 2
Preparation of 1 L of Tris–HCl-buffered SBF with 27 mM HCO_3^- [13,14]

Order	Reagent	Amount (gpl)	Ion	Human plasma (mM)	*Tris*–SBF with 27 mM HCO_3^- (mM)
1	NaCl	6.547	Na^+	142	142
2	$NaHCO_3$	2.268	Cl^-	103	125
3	KCl	0.373	HCO_3^-	27	27
4	$Na_2HPO_4{\cdot}2H_2O$	0.178	K^+	5	5
5	$MgCl_2{\cdot}6H_2O$	0.305	Mg^{2+}	1.5	1.5
6	1 M HCl	15 mL	Ca^{2+}	2.5	2.5
7	$CaCl_2{\cdot}2H_2O$	0.368	HPO_4^{2-}	1	1
8	Na_2SO_4	0.071	SO_4^{2-}	0.5	0.5
9	$(CH_2OH)_3CNH_2$	6.057			
10	1 M HCl	Titrate to pH 7.4 at 37 °C			

KCl is only used to maintain the K concentration at 5 mM in the resultant solution. The use of calcium chloride dihydrate, instead of calcium chloride anhydrous, will also help to eliminate the measuring errors (in each preparation batch) to be caused by using a highly hygroscopic material. Table 2 gives the detailed preparation recipe for Tris–HCl-buffered 1×SBF solution with 27 mM HCO_3^-. Preparation of Tris–HCl-buffered 1.5×SBF solutions with a HCO_3^- concentration of 40.5 mM was recently described elsewhere [17]. 1.5×SBF solutions are generally used in rapid coating of CaP onto many different substrates, as well together with 5×SBF [19] or 10×SBF solutions [20].

2.2. Preparation of collagen–carbonated apatitic CaP composites

Approximately three millimeter-thick bioresorbable collagen membranes or sponges (i.e., Matrix Collagen Sponge™) were obtained from Collagen Matrix, Inc. (Franklin Lakes, NJ, USA), and used as-received after cutting those into 1×1×0.3 cm coupons [21]. These sponges were consisting of purified Type I collagen (which in turn is rich in glycine, proline, and hydroxyproline) in its native triple helical structure. Composites of collagen–carbonated apatitic CaP were synthesized by simply soaking these collagen sponges in a Tris–HCl-buffered SBF solution of 27 mM HCO_3^- (abbreviated as "Tris–SBF-27 mM") for 7 days at 37 °C. One collagen sponge was placed into a clean Pyrex® media bottle (of 100 mL-capacity) and then 75 mL of freshly prepared Tris–SBF-27 mM solution was poured into the bottle, followed by sealing the bottle tightly with its screw cap. The bottle was placed into a microprocessor-controlled oven at 37 °C. The solution was replenished at every 48 h with a fresh, unused Tris–SBF-27 mM solution. At the end of 7 days of soaking, the sponges were gently washed with an ample supply of deionized water, placed into glass Petri dishes, and dried overnight at 37 °C in air. Tris–HCl-buffered 1.5×SBF solutions of 40.5 mM HCO_3^- solutions (Tris–SBF-40.5 mM) may also be used to accelerate the process.

2.3. Preparation of biomimetic and carbonated CaP microrods

The details of CaP microrod preparation were reported elsewhere in greater detail [22]. Briefly, aqueous solutions containing dissolved $NaNO_3$, $Ca(NO_3)_2{\cdot}4H_2O$, KH_2PO_4, concentrated HNO_3, and urea (all reagent-grade, Fisher Chemicals, Fairlawn, NJ) were prepared in 10 mL of deionized water in 30 mL-capacity Pyrex® beakers, as shown in Table 3.

The first chemical added to the beakers was $NaNO_3$, while the last one was urea. Small aliquots of concentrated HNO_3 were added to dissolve back any colloidal precipitates that might have formed following the addition of $Ca(NO_3)_2{\cdot}4H_2O$ and KH_2PO_4 into the $NaNO_3$ solution. For each case shown in Table 3, clear-transparent solutions were thus obtained. Sample beakers were then placed onto 10×10×1 cm alumina insulating fiberboards and covered with an upside down 250 mL-capacity glass beaker. To proceed with the synthesis process, the above-mentioned sample assemblies were placed into a household microwave (MW) oven (Sunbeam, max. power 600 W, 2.45 GHz, Boca Raton, FL) for only 5 min. The MW oven was operated at its maximum power setting. At the end of 5 min of MW heating, the sample beakers reached a temperature of about 500° to 550 °C and were slowly cooled to room temperature (RT), in the MW oven, during the next 20 min. The substance in the sample beaker was then placed into 500 mL of deionized water at RT (22±1 °C) and stirred with a Teflon-coated magnetic fish on a stirrer at around 300 rpm for 1 h, immediately followed by filtration (No. 42 filter paper, Whatman Int. Ltd., Maidstone, England) in a vacuum-assisted Buechner funnel and washing with 2 L of water. At the end of filtration the effluent solutions were transparent and free of whiskers. Samples were dried at 80 °C in air overnight.

In this study we only report the formation of biomimetically synthesized CaP microrods upon soaking the above-mentioned HA microrods in Tris–SBF-27 mM solutions, whereas the behavior of TCP and biphasic HA-TCP microrods soaked in a Tris–SBF-27 mM solution was discussed elsewhere [23]. To synthesize the biomimetic CaP microrods, 500 mg portions of HA whiskers (in powder form) were placed into clean Pyrex® media bottles (of 100 mL-capacity) and then 75 mL of freshly prepared Tris–SBF-27 mM solutions were poured into the bottles. The rest of the Tris–SBF-27 mM soaking practices were performed for 7 days at 37 °C, in a manner very similar to that described above for the collagen sponges.

2.4. Preparation of monetite ($CaHPO_4$)-doped calcium sulphate composites

$CaHPO_4$ (DCPA; dicalcium phosphate anhydrous; catalog No: 1430-01, J. T. Baker, Phillipsburg, NJ)-doped calcium sulfate cement samples were prepared and studied over the composition range of 5 to 33 wt.% $CaHPO_4$ [24]. For

Table 3
Preparation of HA, TCP, and biphasic HA-TCP microrods [22]

Sample	$NaNO_3$ (g)	$Ca(NO_3)_2{\cdot}4H_2O$ (g)	KH_2PO_4 (g)	15.69 M HNO_3 (mL)	Urea (g)	Molar Ca/P
HA	5	1	0.345	0.1	1.75	1.67
TCP	5	1	0.384	0.1	–	1.50
Biphasic HA-TCP	5	1	0.345	0.1	0.075	1.67

the preparation of, for instance, 33 wt.% $CaHPO_4$–67% CSD samples, 1.0 g of $CaHPO_4$ and 2.0 g of CSH (Catalog No: 307661, Sigma-Aldrich, St. Louis, MO) powders were first dry mixed in an agate mortar for 30 min. Powders were then kneaded for 150 s, by using an agate pestle, with 1.2 mL of deionized water (i.e., resultant Liquid-to-Powder (L/P)= 0.40 mL/g) in the same mortar. Thus formed paste was immediately transferred into a cylindrical stainless steel die with a diameter of 12.7 mm, followed by inserting a stainless steel plunger of almost the same diameter into the paste-filled die cavity. A rectangular steel block weighing exactly 9.979 kg was placed on that plunger for 30 s. In other words, this practice corresponded to the reproducible application 0.079 kg/mm^2 (=0.775 MPa) of static load on the wet paste to form a typical cement cylinder. By this way, cement cylinders of 12.7 mm diameter and 15 mm height were formed. The diameter and length of each sample were accurately measured by using a micrometer. Cylinders were then pushed out of the dies by using the same plunger. These cylinders were stored overnight at room temperature (RT: 22±1 °C) in air at a relative humidity of about 70% until further characterization tests. To test the apatite-inducing ability of the samples of this study, pellets (12.7 mm diameter, 15 mm height) of pure CSD and $CaHPO_4$-doped CSD cements were both soaked in 100 mL-capacity glass bottles (one pellet per bottle) containing 75 mL of Tris–SBF-27 mM solutions for 7 days at 37 °C. The Tris–SBF-27 mM soaking practices were very similar to those described above for the biomimetic CaP microrods. Mechanical testing (i.e., the load versus displacement curves) was performed using a Universal Testing Machine (Instron, Phoenix 20K, MTI, Roswell, GA). The cylinders were placed between self-leveling plates and compressed at 1 mm/min. Load was applied until failure of the specimen occurred. Diametral tensile strength (DTS) values were also calculated by using the following formula [25,26]:

$$\alpha\ (\mathrm{DTS}) = 2P/\pi dh \quad (1)$$

where P was the applied load in compression, d was the diameter, and h was the height of cylinders which were tested in triplicate.

2.5. Sample characterization

Phases present in the samples were determined by using a powder X-ray diffractometer, XRD, (XDS 2000, Scintag, Sunnyvale, CA) operated at 40 kV and 30 mA with monochromated Cu K_α radiation. The XRD spectra of CaP-coated collagen sponge coupons were collected after mounting those directly into the sample holders. CaP microrod and calcium sulfate samples were crushed and ground into a fine powder prior to XRD runs, then sprinkled onto the single crystal quartz flat sample holders which were made sticky by applying a very thin layer of vaseline, and the XRD data were collected by using a step size of 0.03 and preset time of 1 s. Fourier Transformed Infrared Spectroscopy, FTIR (Nicolet 550, Thermo-Nicolet, Woburn, MA) data were collected on the samples. FTIR samples were first ground (with the exception of collagen sponges, whose IR spectra were collected by using an ATR–FTIR apparatus in the contact mode) in a mortar, in a manner similar to that used in the preparation of XRD samples, then mixed with KBr powder in a ratio of 1:100, followed by forming a pellet by using a uniaxial cold press. 128 scans were performed at the typical resolution of 3 cm^{-1}. The microstructure of the external or fracture surfaces of the samples and powders was observed by using field-emission scanning electron microscopy, FESEM (S-4700, Hitachi, Tokyo, Japan). Platinum sputtering was used, prior to the FESEM studies, to render the sample surfaces conductive. The BET surface area of powder samples was determined by applying the standard Brunauer–Emmett–Teller method to the nitrogen adsorption isotherms obtained at −196 °C using an ASAP 2020 instrument (Micromeritics Corp., Norcross, GA).

3. Results and discussion

SBF solutions of pH 7.4 were currently used in experimental studies (performed at the human body temperature of 37 °C) for coating titanium/Ti–6Al–4V, nickel–titanium alloys, tantalum, certain polymers or ceramics with a thin layer of carbonated apatitic CaP [17,20,27]. This way of forming biocompatible CaP deposits was called biomimetic coating [28,29]. The apatitic CaP-inducing ability of a material having an abundance of surface-bound OH (hydroxyl) groups immersed in an SBF solution stood for (i) the OH groups to upset the local pH balance of the SBF solution and (ii) the same to cause the aggregation of Posner's nanoclusters (already present in an otherwise transparent SBF solution [20,30–32]) into visibly large precipitates. Al_2O_3 or ZrO_2 ceramics immersed into an SBF solution will not form CaP deposits on them (i.e., no biomimetic coating). However, if the same ceramics were first boiled in a strong NaOH or KOH solution for several days, they will start showing the first signs of biomimetic CaP coating. Uchida et al. [33] explained this by the incorporation of Zr–OH or Al–OH groups onto the surfaces of ceramic samples by boiling in strong alkali solutions. In the case of titanium and its alloys, soaking the metal coupons at 60–70 °C in NaOH [5] or KOH [20] solutions, overnight, would easily render them "able-to-induce-CaP-deposits" upon soaking in a Tris–SBF-4.2 mM [5] or Tris–SBF-27 mM [13] solution.

Concentration and availability of carbonate ions in SBF solutions were shown to have a noteworthy role on the incubation of carbonated, apatitic mineralites [34,35]. An SBF solution with a significant deficiency in its HCO_3^- concentration (such as, 4.2 mM [4,5]) takes a significantly longer time in nucleating CaP mineralites than could be achieved by using an SBF solution with 27 mM HCO_3^- [35,36]. On the other hand, the ability of a material to form CaP on its surface upon immersion in an SBF solution does not necessarily mean that that material will take part in bone remodeling and biodegradation processes *in vivo*. Clinicians usually prefer biodegradable and absorbable materials in treating bone defects [37].

The use of Tris–SBF-27 mM solution as a medium of bulk synthesis, instead of pure water, was previously shown to be a viable alternative to produce (i) substituted (with elements such

as Na, K, Mg, which are present in human bones) biomimetic apatites, and (ii) nanoapatites of extremely small particle sizes (<25 nm) and of high surface areas in excess of 100 m^2/g [13,14,38,39]. The use of enzyme urease-catalyzed decomposition of urea added to Tris–SBF-27 mM solutions was also shown to work well in stabilizing the pH of SBF solutions at around 7.4 (at 37 °C) during the preparation of nanoapatites in bulk quantities [40]. Therefore, the Tris–SBF-27 mM solution can be used to transform certain materials into bone-like calcium phosphates and implantable medical devices. The experimental case studies reported below would hopefully help in describing the extent of the above-mentioned biomimetic transformation achieved by this solution having 27 mM HCO_3^-.

3.1. Composites of collagen and apatitic CaP

Collagen is the *de facto* biopolymer in mammalians, whereas cellulose is that of plants and trees, and chitin is seen in the exoskeleton of crustaceans (sea-shells, oysters, crabs, etc.). Human bones are meticulous composites of collagen and carbonated, apatitic CaP mineralites. Collagen is tough and inextensible, with great tensile strength, and is the main component of cartilage, ligaments, tendons, and bones [41]. Multiple tropocollagen (with triple helix structures) molecules (300 nm long and 1.5 nm in diameter) form collagen fibrils, and multiple collagen fibrils form collagen fibers [42]. Soaking of collagen membranes or sponges in Tris–SBF-4.2 mM solution was first studied and reported by Rhee and Tanaka [43]. Lickorish et al. [44] later confirmed the findings of Rhee and Tanaka [43]. Girija et al. [45] tested the viability of a Hepes–NaOH-27 mM SBF solution [46] in synthesizing collagen–CaP composites by soaking fibrous collagen in that solution. Collagen–apatitic CaP composites are, therefore, seen as ideal bone substitutes.

The micromorphology of the as-received collagen sponges was depicted in the electron micrograph of Fig. 1(A). Sponges comprised a cellular structure, with cell (i.e., pore) sizes varying from 200 to 450 μm. Fig. 1(B) showed the extensive coverage on the cell walls of the collagen sponge coupons with carbonated, apatitic CaP upon 7 days of soaking those in Tris–SBF-27 mM solution at 37 °C. After SBF soaking, the pore sizes still remained in the same range. The inset in Fig. 1(B) displayed the nanotexture possessed by apatitic CaP formed on collagen in this specific SBF solution. The Tris–SBF-4.2 mM solution of the previous studies [43,44] was not able to provide the extent of coverage observed in this work. Low HCO_3^- concentration of the Tris–SBF-4.2 mM solution was the culprit. The ATR-contact–FTIR traces shown in

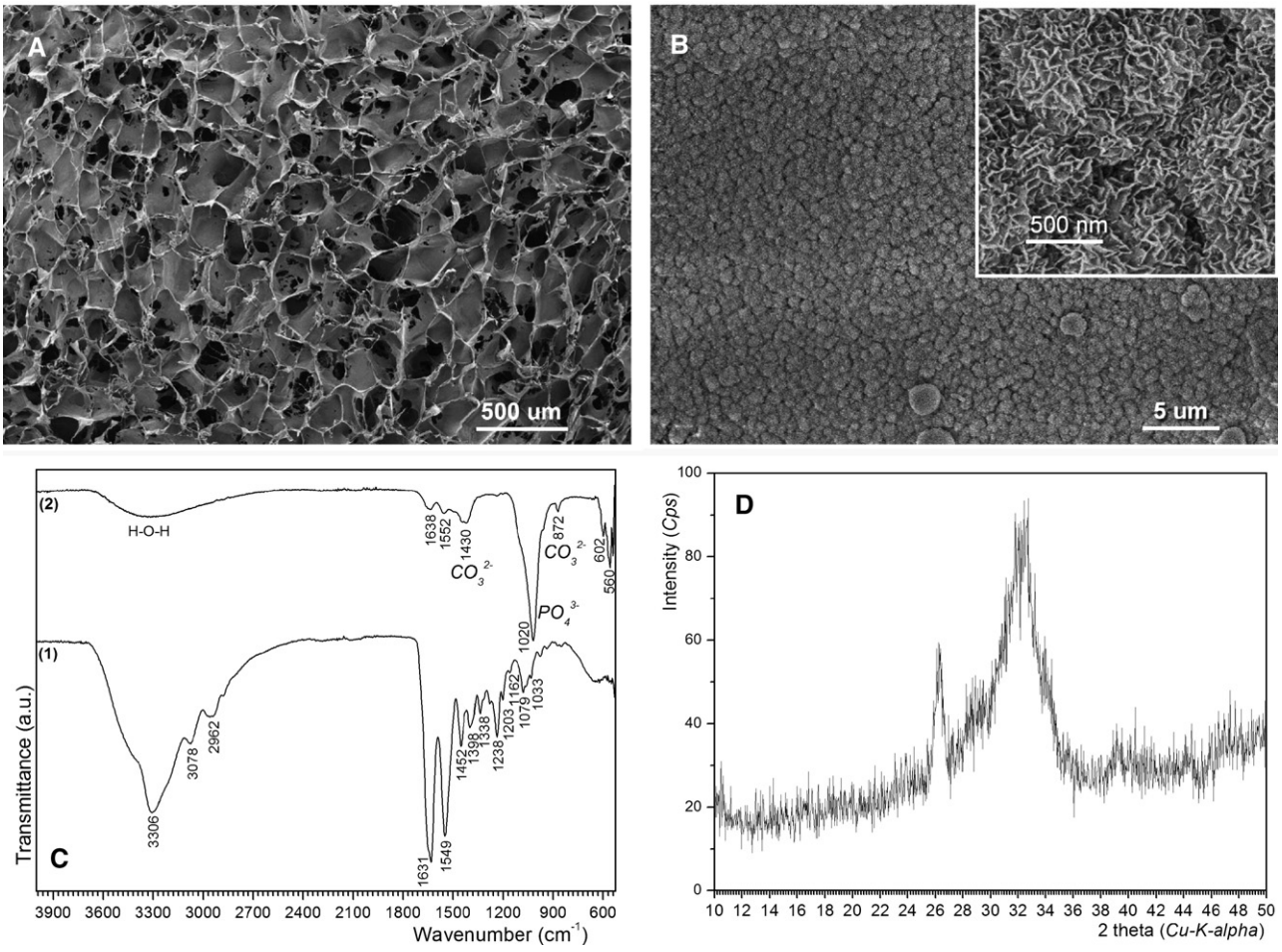

Fig. 1. (A) SEM micrograph of *as is* collagen sponge coupons; (B) collagen coupon after 1 week of soaking at 37 °C in Tris–SBF-27 mM; (C) FTIR traces of collagen coupons, (1) pristine, (2) SBF-soaked; (D) XRD trace of SBF-soaked collagen coupon.

Fig. 1(C) gave another proof of the extensive coverage of the collagen fibrils of the coupons by the carbonated, apatitic CaP phase. Trace (1) of Fig. 1(C) belonged to the pristine collagen coupons, whereas trace (2) of the same figure displayed a remarkable decrease in the intensities of amide bands after Tris–SBF-27 mM immersion.

XRD chart of a sample collagen–apatitic CaP composite coupon was shown in Fig. 1(D), it was characteristic for the nanocrystalline (or poorly crystallized) nature of apatitic CaP formed in aqueous solutions of neutral pH. The data of Fig. 1(D) was collected from a Tris–SBF-27 mM-soaked coupon after placing it directly on the sample holder of the diffractometer.

Pompe et al. [47,48] have reported an alternative route to synthesize composites of collagen and apatitic CaP in which collagen was first dissolved in a highly acidic solution of $CaCl_2$, followed by neutralization at pH 7 (37 °C) by using a Tris-buffered phosphate solution. Such a route shall be regarded as the mineralization of discrete CaP particles attached onto the collagen fibrils, and indeed the experimental electron photomicrographs of this technique proved this point [47]. It should be noted that the chemical nature of the nucleating apatitic solid phase (which contains Na, K, and Mg, as well) from an SBF solution and that of the CaP produced from a pure $CaCl_2$–HPO_4^{2-} solution mixture [47,48] is quite different. The term biomimetic mineralization should rather be reserved for the former.

The synthesis procedure described here has the advantage of near-net shape processing. Collagen coupons immersed into the Tris–SBF-27 mM solution retained their dimensions after 1 week at 37 °C. This was mainly due to the nucleation of the apatitic CaP globules within the first few hours of soaking, helping to significantly restrain the swelling of collagen. BET surface areas of the *as is* collagen coupons were measured to be 26 ± 2 m^2/g, whereas after SBF soaking this value increased to 64 ± 3 m^2/g. High surface area osteogenic biomaterials are strongly needed for improved bone cell (i.e., osteoclasts and osteoblasts) attachment and proliferation, as well as for the subsequent positive *in vivo* performance.

3.2. Biomimetic CaP microrods

The synthesis of whiskers, short fibers or single crystals of bone-compatible calcium phosphates (i.e., with the exclusion of highly acidic calcium phosphates, such as $Ca(H_2PO_4)_2$ and $Ca(H_2PO_4)_2{\cdot}H_2O$) has received an increasing amount of attention over the course of last two decades. The main incentive behind these efforts was the hope of overcoming the inherent mechanical weaknesses of synthetic calcium phosphates. The reinforcement of weak CaP bioceramics with whiskers or short fibers of the same was thought to be a remedy. The pioneering work of Yubao et al. [49], Yoshimura et al. [50] and Iizuka et al. [51] on the hydrothermal synthesis of CaP whiskers exemplified extremely facile methods to produce heavily agglomerated bundles of short fibers. We have previously described a molten salt technique which made it possible, for the first time, to synthesize perfectly monodisperse, agglomerate-free whiskers of Ca-hydroxyapatite ($Ca_{10}(PO_4)_6(OH)_2$) [52,53]. The interfacial bonding–debonding mechanisms between smooth-surfaced CaP fibers/whiskers and the CaP matrices were unfortunately found to be the strength-limiting issue in whisker-reinforced CaP matrix composites. There arose the need for synthesizing CaP short fibers or rods with rough surfaces.

Hydroxyapatite microrods with smooth surfaces were first synthesized by using a microwave-assisted molten salt procedure [22], as shown in Fig. 2(A). Upon soaking in Tris–SBF-27 mM solution for 1 week, these microrods (9 m^2/g surface area, initially) transformed into rods of higher surface area (45 m^2/g), Fig. 2(B) and (C) [23]. XRD and FTIR characterization of these rods, together with their *in vitro* osteoblast cell attachment and

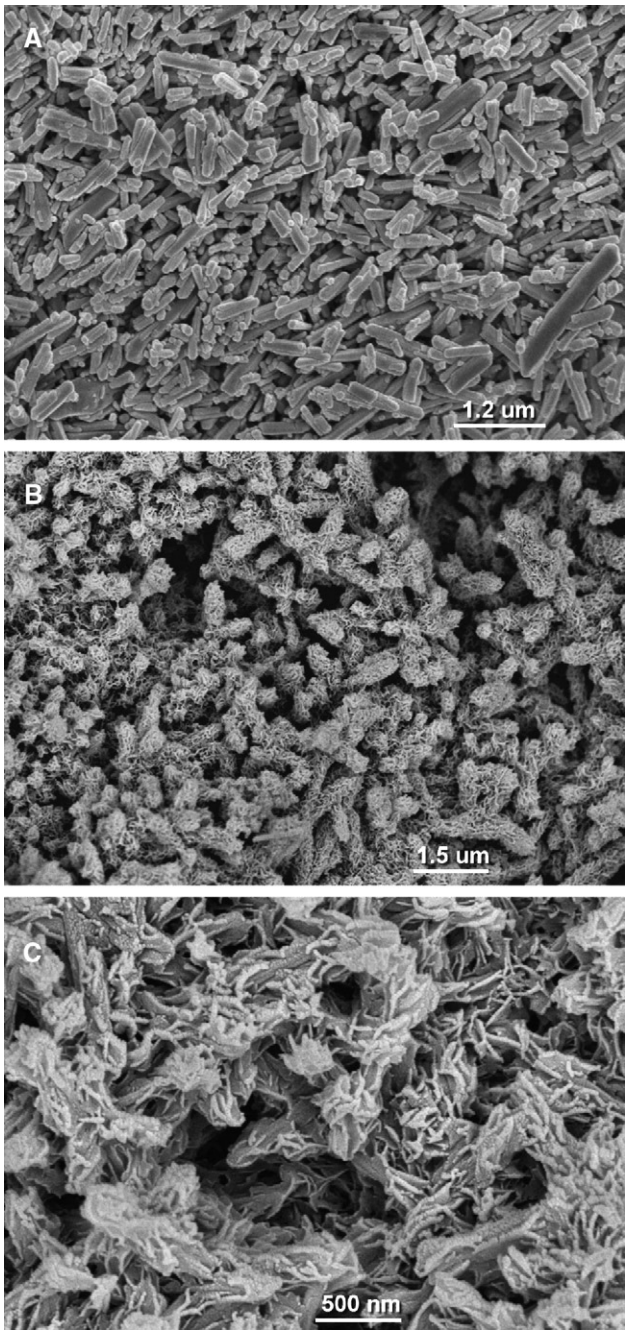

Fig. 2. SEM photomicrographs of hydroxyapatite microrods: (A) pristine rods; (B) and (C) after soaking in Tris–SBF-27 mM solution for 7 days.

proliferation tests, were reported elsewhere [23]. The pristine apatitic microrods were not totally stable or completely insoluble in Tris–SBF-27 mM solution. This was the reason why their morphology changed during SBF soaking. However, Tris–SBF-27 mM solution did not just precipitate or attach some semi-spherical CaP globules (or spherulites) on these neat microrods, but during soaking, the microrods went through a process of low level surface dissolution–reprecipitation and thus maintained their rod-like shapes. These microrods of high surface area are also expected to find uses in the manufacture of novel bio-polymer–CaP composites.

3.3. $CaHPO_4$-doped calcium sulfate + phosphate composites

Calcium sulfate cement pastes or pre-formed pellets are in clinical use as bone graft substitute materials of high *in vivo* solubility [54,55]. The formation of such cements is based on the rapid reaction of calcium sulfate hemihydrate (CSH, $CaSO_4 \cdot 1/2H_2O$) with water to form calcium sulfate dihydrate (CSD, Gypsum, $CaSO_4 \cdot 2H_2O$) as the reaction product. In many cases, calcium sulfate bone substitutes are degraded and absorbed before the *in vivo* invasion and repair of the bone defect by the natural bone [56,57].

Calcium sulfate hemihydrate (CSH, $CaSO_4 \cdot 1/2H_2O$) powders, when mixed with water, readily convert into calcium sulfate dihydrate (CSD, Gypsum, $CaSO_4 \cdot 2H_2O$). Surgical grade calcium sulfate, following its FDA approval, is currently marketed to the orthopedic surgeons as a bone repair material [58–61]. Calcium sulfate is a highly biocompatible material that has the characteristic of being one of the simplest synthetic graft materials. Moreover, crystallized CSD was considered to be osteogenic *in vivo* [62–65]. However, calcium sulfate cements might have few points of concerns: (*i*) they undergo rapid passive dissolution and exhibit high rates of *in vivo* resorption even before the host bone has had time to grow into the defect area [57]; (*ii*) cytotoxic effect: their rapid dissolution leads to slightly acidic cytotoxic micro-environments responsible for local inflammatory processes (such as, fibroblast encapsulation) to take place at the site of implantation [56]. While inflammatory tissues were found to disappear after 60 days in bone, they remained in soft tissue implantation sites of white New Zealand rabbits [66]; (*iii*) pure calcium sulfate is not able to maintain its initial dry strength; it disintegrates; and (*iv*) pure calcium sulfate does not have the property of osteoconductivity. To address these concerns and to improve the properties of calcium sulfate cements, calcium phosphate additions (β- and α-TCP ($Ca_3(PO_4)_2$; tricalcium phosphate), HA ($Ca_{10}(PO_4)_6(OH)_2$; hydroxyapatite) and $Ca(H_2PO_4)_2 \cdot H_2O$) have already been investigated by previous researchers [57,67–69].

To the best of our knowledge, the physical addition of $CaHPO_4$ (monetite) to CSH powders, to get easy-to-produce phosphate + sulfate composite bone cements, has not been studied before. $CaHPO_4$ is one of the most soluble calcium phosphate phases [70], and is clinically used as a minor powder component in calcium phosphate cements designed for skeletal and dental repair [71]. The characteristic XRD trace of the starting material, monoclinic α-$CaSO_4 \cdot 1/2H_2O$ (CSH, *Bassanite*) is given in trace (A) of Fig. 3. This experimental pattern (a = 12.028, b = 6.932, c = 12.691 Å, β = 90.183°) resembles to that given in ICDD PDF 41-0224 (International Centre for Diffraction Data, Swarthmore, PA; Powder Diffraction File). β-$CaSO_4 \cdot 1/2H_2O$ (ICDD PDF 45-0848, hexagonal; a = 13.96, c = 12.75 Å) is known as the *plaster of Paris*. The XRD data for the $CaSO_4 \cdot 2H_2O$ (ICDD PDF 06-0046) cements formed after mixing CSH powders with water are given in trace (B) of Fig. 3. CSH is expected to react with water according to the following theoretical reaction

$$CaSO_4 \cdot 1/2H_2O + 3/2H_2O \rightarrow CaSO_4 \cdot 2H_2O \quad (2)$$

This is a well-known cement reaction, but with the stoichiometric water amount indicated above one cannot obtain a malleable and compliant cement paste. This reaction in its stated form occurs very slowly. As such it is not of any practical utility [72]. The "liquid-to-powder" ratio (i.e., L/P ratio) expressed in the form of [mL of setting solution/g of cement powder] is a practical convention used among the cement researchers. The L/P ratio dictated by reaction (2) can easily be calculated as (27.0231 mL H_2O divided by 145.1493 g CSH powder) 0.186. Therefore, the common practice in accelerating this reaction has been doubling the amount of water used, i.e., L/P > 0.35. This is why we have chosen an L/P ratio of 0.40 for a more complete and rapid transformation of CSH into CSD. The data of Fig. 3 confirmed that CSH powders were fully converted into CSD by using the L/P ratio and the experimental conditions of this study. In a similar fashion, Fig. 4 showed the FTIR traces of pure CSH and pure CSD powders. These XRD and FTIR patterns served as controls prior to the experiments on adding $CaHPO_4$ into CSH powders. CSH powders are known to undergo a natural ageing process (i.e., slow conversion into CSD) if they were stored uncovered at room temperature even at a relatively mild humidity level of 65% [73]. Therefore, throughout this study utmost care was practiced not to hydrate the CSH powders during the processing steps. XRD and FTIR spectra of pure $CaHPO_4$ powders are given in Fig. 5(A) and (B), respectively. These data were also used as references in characterizing $CaHPO_4$ + CSH powder and cement mixtures.

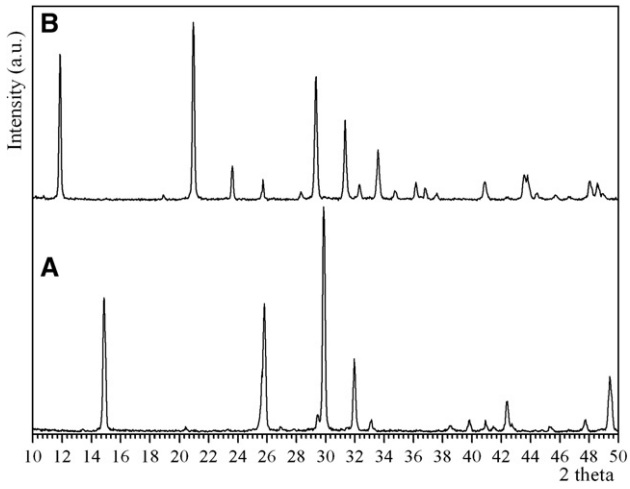

Fig. 3. XRD traces of (A) pure $CaSO_4 \cdot 1/2H_2O$ and (B) pure $CaSO_4 \cdot 2H_2O$.

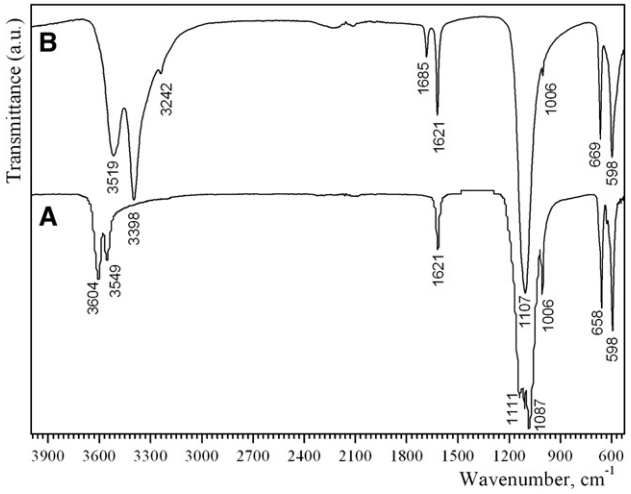

Fig. 4. FTIR traces of (A) pure $CaSO_4 \cdot 1/2H_2O$ and (B) pure $CaSO_4 \cdot 2H_2O$.

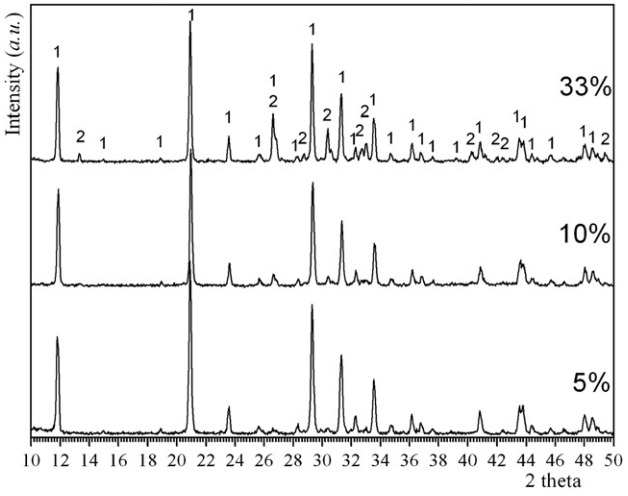

Fig. 6. XRD traces of 5, 10, and 33% $CaHPO_4$-added calcium sulfate cements (1: CSD and 2: $CaHPO_4$ peaks).

The XRD data given in Fig. 6 for 5, 10, and 33% $CaHPO_4$-added calcium sulfate samples showed that in all of these the presence of $CaHPO_4$ did not hinder the full conversion of CSH into CSD. In direct comparison with Fig. 3(A), the traces of Fig. 6 did not show any unreacted CSH. $CaHPO_4$ has a triclinic unit cell with the following lattice parameters: $a=6.910$, $b=6.627$, $c=6.998$ Å, $\alpha=96.34°$, $\beta=103.82°$, and $\gamma=88.33°$. Its structure consists of $CaHPO_4$ chains held together by Ca–O bonds and three types of hydrogen bonds [74]. The dissolution kinetics of $CaHPO_4$ in water at 37 °C has been previously investigated by Lebugle et al. [75]. This study showed that calcium and phosphate ions were released from $CaHPO_4$ with time and stopped after 4 days in contact with water at 37 °C [75]. The Ca/P atomic ratio in water, in which the dissolution study was performed, also decreased with time and was 0.75 after 15 min of dissolution; it finally reached a value of 0.62. The dissolution of DCPA was found to be incongruent [75]. This incongruency can be explained by the formation of a thin apatitic calcium phosphate layer on the surfaces of $CaHPO_4$ particles through a topotactic reaction, which hindered further dissolution. The logarithm of the thermodynamic solubility (i.e., log K_{sp}) of $CaHPO_4$ was reported by McDowell et al. [76] to be −6.90 and −7.04 at 25 °C and 37 °C, respectively. K_{sp} of $CaHPO_4$ is defined by Eq. (3)

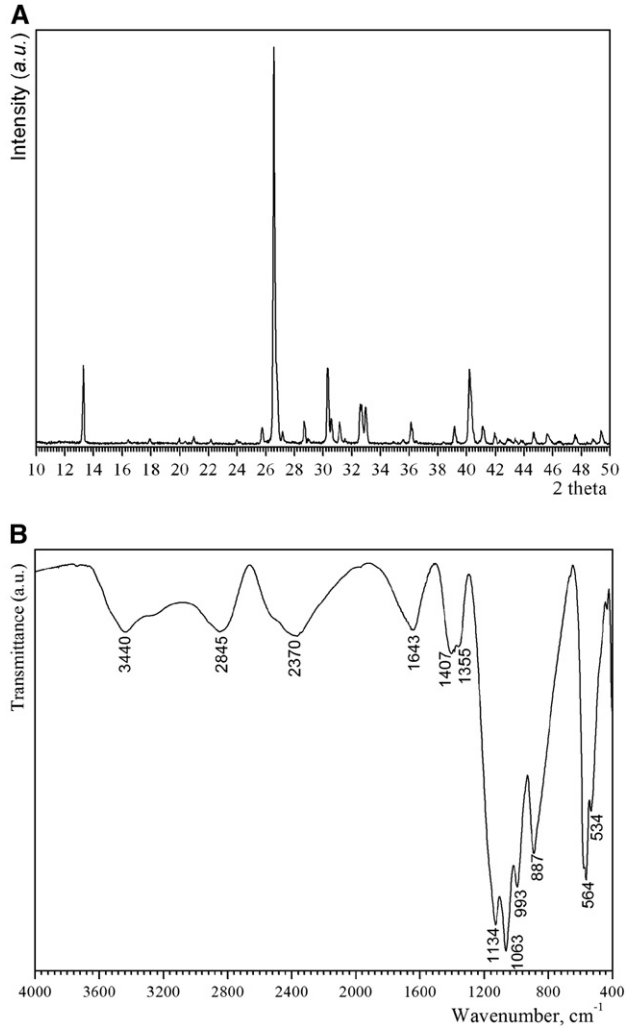

Fig. 5. XRD (A) and FTIR (B) data for pure $CaHPO_4$ powders.

$$CaHPO_{4(s)} \rightarrow Ca^{2+}_{(aq)} + HPO^{2-}_{4\,(aq)},\ K_{sp} = [Ca^{2+}][HPO^{2-}_4] \quad (3)$$

For comparison purposes, K_{sp} values for $CaHPO_4 \cdot 2H_2O$ (*brushite*), $CaCO_3$, $Ca_{10}(PO_4)_6(OH)_2$ (*hydroxyapatite*), $Ca_3(PO_4)_2$ (*whitlockite*), and $Ca_9(HPO_4)(PO_4)_5(OH)$ (*Ca-deficient hydroxyapatite*) are known to be −6.59, −8.55, −117.1, −81.7, and −85.1, respectively [77]. These numbers simply indicated the solubility of a specific substance; for example, stoichiometric hydroxyapatite (−117.1) was therefore much less soluble than Ca-deficient hydroxyapatite (−85.1). Gypsum (CSD) has a monoclinic unit cell with the lattice parameters: $a=5.678$, $b=15.213$, $c=6.286$ Å, $\beta=114.08°$ [78,79]. The logarithm of the solubility product for CSD is −4.58 [80], which means that CSD is more soluble than $CaHPO_4$ (−6.90).

Fig. 7 depicted the FTIR traces of 5, 10, and 33% $CaHPO_4$-added calcium sulfate samples. Interestingly, the IR spectra were all similar to that of CSD. The shoulder-like bands over the

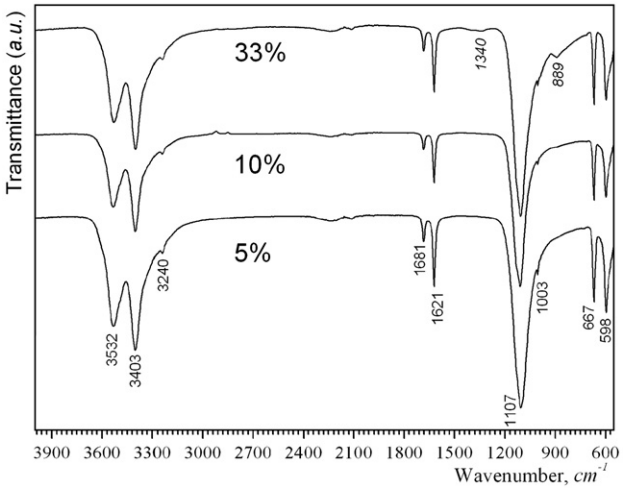

Fig. 7. FTIR traces of 5, 10, and 33% $CaHPO_4$-added CSD cements.

range of 1360 to 1290 cm^{-1}, which appeared only in the top IR trace (i.e., 33 wt.% $CaHPO_4$) of Fig. 7, were due to the HPO_4^{2-} groups [81]. Characteristic IR bands of pure $CaHPO_4$ are located at 2803, 2326, 2110, 1630, 1399, 1345, 1124, 1060, 986, 884, 555 and 535 cm^{-1}, as shown in Fig. 4(B). The bands at 555–535 and 884 cm^{-1}, which can also be ascribed to $CaHPO_4$, were only slightly visible even in the 33% $CaHPO_4$-added samples. 5 and 10% $CaHPO_4$-added samples did not clearly reveal those distinct bands.

Morphology of the starting powders, i.e., pure $CaHPO_4$ and pure CSD, was shown in Fig. 8(A) and (B), respectively. CSD shown in Fig. 8(B) was the reaction product of CSH and water. CSH powders (not shown) consisted of gravel-shaped particles in the range of 5 to 50 μm. Those characteristic "gravels" [82] of CSH were microporous, as well. $CaHPO_4$ powders (Fig. 8)(A), on the other hand, comprised of rectangular prismatic particles, over the size range of 10 to 25 μm, with a smaller overall particle size distribution than that of CSH. The CSH to CSD transformation totally consumed these large particles of CSH, and resulted in the formation of submicron-thick CSD short whiskers, as shown in Fig. 8(B). These CSD needles (Fig. 8(B)) intermingling with one another explained the strength development in these samples. According to the Gillmore needle test results, pure CSD cylinders of this study, when mixed with deionized water at the L/P ratio of 0.375, had a t_i of 21±2 min and a t_f of 32±3 min. As reported by Carlson et al. [83] for instance, the use of a lower L/P ratio, such as 0.32, with pure CSH powders would have lowered these t_i and t_f values down to 17 and 25 min, respectively. On the other hand, 5, 10, and 33% $CaHPO_4$-added CSD samples did not yield a measurable change in the above-mentioned t_i and t_f values of pure CSD.

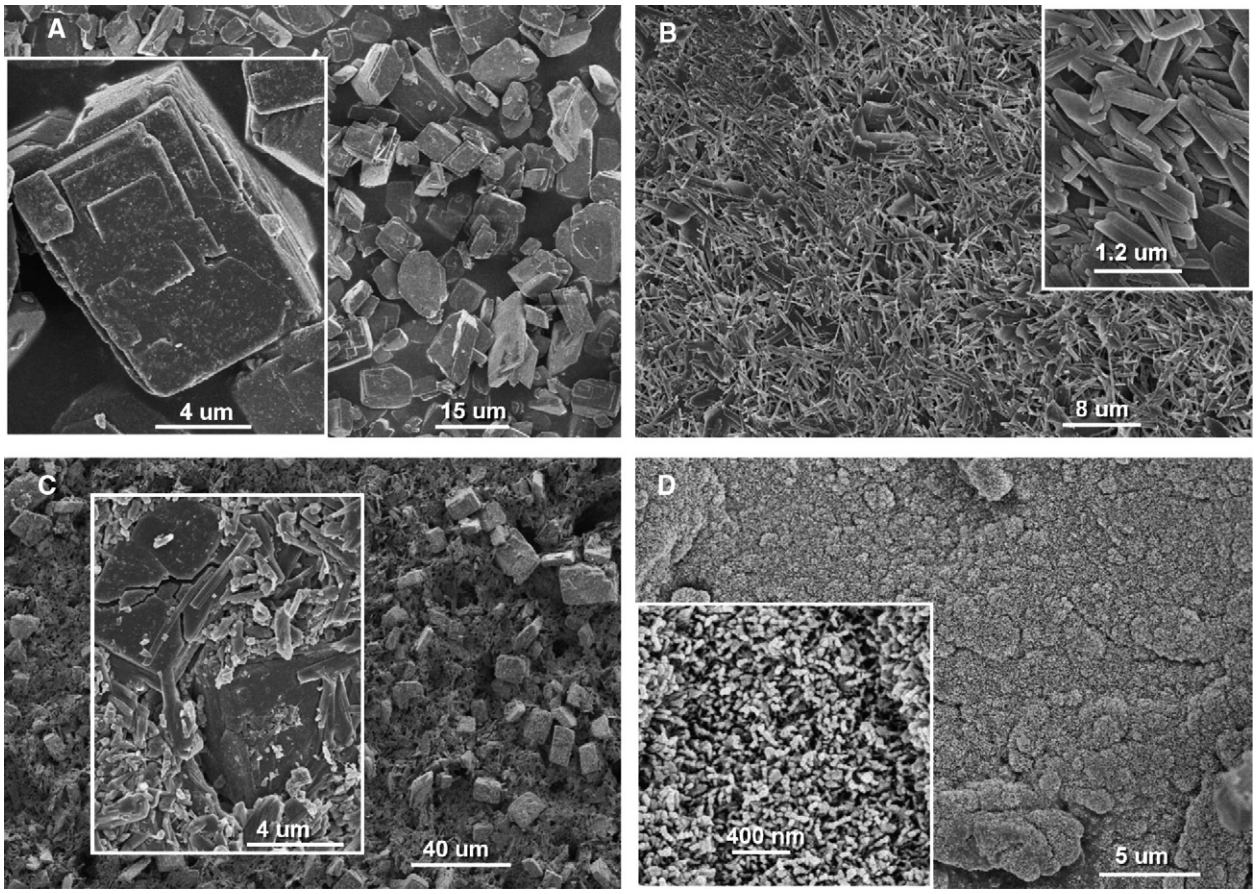

Fig. 8. SEM micrographs of (A) pure $CaHPO_4$ powders, (B) pure CSD cement surface, (C) 33% $CaHPO_4$–67% CSD cement, prior to Tris–SBF-27 mM soaking, and (D) 33% $CaHPO_4$–67% CSD cement, after Tris–SBF-27 mM soaking for 1 week at 37 °C.

After soaking the pure CSD and $CaHPO_4$-doped CSD pellets in Tris–SBF-27 mM solution for 1 week at 37 °C, the most interesting observation was the total collapse of the pure CSD pellet into a powder. There was no apatitic CaP formation observed on the surfaces of those crumbled CSD whisker bundles. However, 5, 10, 20, and 33% $CaHPO_4$-added CSD samples did retain their pellet forms at the end of the same soaking runs. The SEM investigations of the surfaces of the 5% through 20% $CaHPO_4$-added calcium sulfate samples also showed no apatitic CaP formation after soaking in Tris–SBF-27 mM for 1 week. It was apparent that these samples (like the pure CSD) did not have an apatite-inducing ability. Fig. 8(C) showed the surface of a 33%$CaHPO_4$–67%CSD cement sample, prior to Tris–SBF-27 mM soaking.

Fig. 8(D) depicted the microstructure of 33% $CaHPO_4$–67% CSD set cement sample after Tris–SBF-27 mM soaking at 37 °C for 1 week. This was the typical coating morphology of apatitic CaP formed in SBF solutions, with the nanotexture visible in the inset of Fig. 8(D). Therefore, 33%$CaHPO_4$–67% CSD cements revealed, for the first time in calcium sulfate-based resorbable cements, a significant apatite-inducing ability, which was not present at all in pure CSD. According to the SEM investigations, the apatitic coating layer on the sulfate-phosphate cement samples (Fig. 8(D)) had a thickness of about 50 μm. We have also found that with the addition of $CaHPO_4$ into calcium sulfate, the load–displacement curves (under compression, on cylindrical samples having a surface area of 125±4 mm^2) improved considerably with respect to those of pure calcium sulfate cements, as shown in Fig. 9. The load versus displacement curves did not vary from one preparation to the other, and always displayed the positive effect of $CaHPO_4$ additions to the otherwise pure CSD cements. Pure CSD cement cylinders of this study failed under a compressive load of about 90±3 kg, whereas the same value for 33%$CaHPO_4$–67% CSD cements was 188±3 kg. These load values corresponded to the compressive strengths of 7±2 (CSD) and 14±2 ($CaHPO_4$+CSD) MPa, respectively. Diametral tensile strengths calculated by using Eq. (1) and the mean load-at-failure values were 0.34 (=3.35 MPa) and 0.71 kg/mm^2 (=7 MPa) for CSD and $CaHPO_4$+CSD samples, respectively.

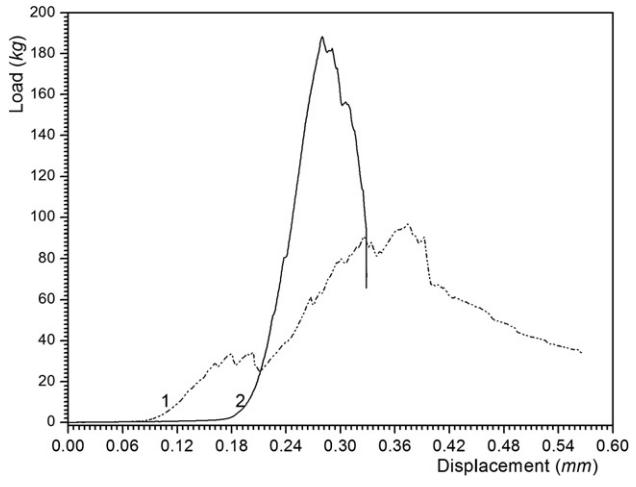

Fig. 9. Comparative load–displacement curves of (1) pure CSD, and (2) 33% $CaHPO_4$–67%CSD set cement cylinders.

CSD samples also showed the characteristic jagged or zigzag behavior in their load versus displacement traces. This was probably due to the porous nature of these samples formed as the result of only physically adhering CSD whiskers, which could easily break loose from one another with an increase in the applied load. It should also be noted that the final compressive and diametral tensile strength values to be obtained in calcium sulfate cements significantly depend on the applied force in forming the cement cylinders. In this study, we were quite conservative in limiting this load to only 0.77 MPa.

Doping of calcium sulfate with $CaHPO_4$ (monetite) seemed to offer several advantages over doping them with hydroxyapatite [84] or α- or β-tricalcium phosphate [85,86] powders to remedy several shortcomings of pristine calcium sulfate samples. The first advantage was that by doping with $CaHPO_4$, one did not need to sacrifice from the overall solubility or *in vivo* biodegradability [87] of the resultant composite material. Log K_{sp} values for hydroxyapatite and tricalcium phosphate are an order of magnitude smaller than that of CSD, whereas that of $CaHPO_4$ is quite similar. Participation of synthetic hydroxyapatite ceramics [88] or α-tricalcium phosphate powders [89] in the natural bone remodeling processes is quite limited. $CaHPO_4$ is the most soluble calcium phosphate phase (with the exclusion of $Ca(H_2PO_4)_2$ and $Ca(H_2PO_4)_2{\cdot}H_2O$, which cannot be used in *in vivo* environments owing to their extreme acidity), and $CaHPO_4$ is already in clinical use in calcium phosphate-based bone cements [89].

The second, and perhaps the most significant, advantage of $CaHPO_4$ addition (beyond a certain level) to the calcium sulfate powders was to impart *in vitro* apatite-inducing ability of the resultant cements. The formation of a nanoporous (i.e., high surface area and high surface reactivity), carbonated, apatitic calcium phosphate layer (which resembles the human bone mineral in this respect [20]) on gypsum-based resorbable pellets can be desirable and may find clinical applications in orthopedic and dental surgery. Moreover, the presence of $CaHPO_4$ (at a level of 33%, as exemplified in this study) in calcium sulfate cements totally prevented the crumbling of the otherwise pure calcium sulfate cement pellets into a fine powder when soaked in Tris–SBF-27 mM solution for 1 week. Rauschmann et al. [84] have recently reported the *in vitro* cytotoxicity of pure calcium sulfate cements to human osteoblast cells. Rauschmann et al. [84] also reported the complete elimination of this cytotoxic effect when they added about 50% hydroxyapatite to the CSH powders. Development of $CaHPO_4$-added calcium sulfate cements, presented for the first time in this study, may exhibit the same positive effect. *In vitro* cell culture studies are certainly needed to verify this speculative argument.

4. Conclusions

(1) Macroporous collagen (Type I) sponges were biomimetically coated with carbonated, apatitic calcium phosphate (Ap-CaP) by using the above-mentioned Tris–SBF-27 mM solution at 37 °C and pH 7.4.

(2) Short whiskers or microrods of apatitic CaP were converted to high surface area, biomimetic CaP microrods by soaking crystalline CaP precursors of rod-like morphology in Tris–SBF-27 mM solution at 37 °C.
(3) 33 wt.% CaHPO4–67 wt.% CaSO4·2H2O cement samples were found to induce carbonated, apatitic CaP formation on their surfaces when soaked in Tris–SBF-27 mM solutions at 37 °C. Pure CaSO4·2H2O samples were not able to form apatitic CaP during the same treatment of soaking in Tris–SBF-27 mM.

Acknowledgements

ACT was a research professor at Clemson University between May 2003 and April 2006. This work was partially supported by the NSF grants 0522057, 0085100 and 0409119.

References

[1] S. Ringer, J. Physiol. 3 (1880–1882) 380.
[2] W. Earle, J.N.C.I. 4 (1943) 165.
[3] J.H. Hanks, R.E. Wallace, Proc. Soc. Exp. Biol. Med. 71 (1949) 196.
[4] T. Kokubo, J. Non-Cryst. Solids 120 (1990) 138.
[5] T. Kokubo, H. Takadama, Biomaterials 27 (2006) 2907.
[6] http://www.sigmaaldrich.com/Area_of_Interest/Life_Science/Cell_Culture/Product_Lines/Classic_Media___Salts.html.
[7] F. Devreker, K. Hardy, M. Van den Bergh, A.S. Vannin, S. Emiliani, Y. Englert, Hum. Reprod. 16 (2001) 749.
[8] C. Karamalegos, V.N. Bolton, Hum. Reprod. 14 (1999) 1842.
[9] A.P. Serro, B. Saramago, Biomaterials 24 (2003) 4749.
[10] L. Frauchiger, M. Taborelli, B.O. Aronsson, P. Descouts, Appl. Surf. Sci. 143 (1999) 67.
[11] M. Metikos-Hukovic, A. Kwokal, J. Piljac, Biomaterials 24 (2003) 3765.
[12] S. Hiromoto, T. Hanawa, K. Asami, Biomaterials 25 (2004) 979.
[13] D. Bayraktar, A.C. Tas, J. Eur. Ceram. Soc. 19 (1999) 2573.
[14] A.C. Tas, Biomaterials 21 (2000) 1429.
[15] A. Oyane, K. Onuma, A. Ito, H.M. Kim, T. Kokubo, T. Nakamura, J. Biomed. Mater. Res. 64A (2003) 339.
[16] M. Ogino, F. Ohuchi, L.L. Hench, J. Biomed. Mater. Res. 14 (1980) 55.
[17] S. Jalota, S.B. Bhaduri, A.C. Tas, J. Mater. Sci., Mater. Med. 17 (2006) 697.
[18] L. Grondahl, F. Cardona, K. Chiem, E. Wentrup-Byrne, T. Bostrom, J. Mater. Sci., Mater. Med. 14 (2003) 503.
[19] P. Habibovic, F. Barrere, C.A. van Blitterswijk, K. de Groot, P. Layrolle, J. Am. Ceram. Soc. 85 (2002) 517.
[20] A.C. Tas, S.B. Bhaduri, J. Mater. Res. 19 (2004) 2742.
[21] http://www.collagenmatrix.com/index.htm.
[22] S. Jalota, A.C. Tas, S.B. Bhaduri, J. Mater. Res. 19 (2004) 1876.
[23] S. Jalota, S.B. Bhaduri, A.C. Tas, J. Biomed. Mater. Res. 78A (2006) 481.
[24] J.N. Swaintek, C.J. Han, S.B. Bhaduri, A.C. Tas, Self-setting orthopedic cement compositions based on $CaHPO_4$ additions to calcium sulphate, in: M. Mizuno (Ed.), Advances in Bioceramics and Biocomposites, The American Ceramic Society, USA, 2005, p. 79.
[25] G.C. Santos, O. El-Mowafy, J.H. Rubo, J. Prosthet. Dent. 91 (2004) 335.
[26] L.C. Chow, S. Hirayama, S. Takagi, E. Parry, J. Biomed. Mater. Res. 53B (2000) 511.
[27] T. Kokubo, Acta Mater. 46 (1998) 2519.
[28] Y. Abe, T. Kokubo, T. Yamamuro, J. Mater. Sci., Mater. Med. 1 (1990) 233.
[29] M. Tanahashi, T. Yao, T. Kokubo, M. Minoda, T. Miyamoto, T. Nakamura, T. Yamamuro, J. Am. Ceram. Soc. 77 (1994) 2805.
[30] A.S. Posner, F. Betts, Acc. Chem. Res. 8 (1975) 273.
[31] A. Oyane, K. Onuma, T. Kokubo, A. Ito, J. Phys. Chem., B 103 (1999) 8230.
[32] G. Treboux, P. Layrolle, N. Kanzaki, K. Onuma, A. Ito, J. Phys. Chem., A 104 (2000) 5111.
[33] M. Uchida, H.M. Kim, T. Kokubo, M. Nawa, T. Asano, K. Tanaka, T. Nakamura, J. Biomed. Mater. Res. 60 (2002) 277.
[34] X. Lu, Y. Leng, Biomaterials 26 (2005) 1097.
[35] S. Jalota, S.B. Bhaduri, A.C. Tas, Mater. Sci. Eng., C 27 (2006) 432.
[36] C. Garcia, S. Cere, A. Duran, J. Non-Cryst. Solids 352 (2006) 3488.
[37] A.F. Schilling, W. Linhart, S. Filke, M. Gebauer, T. Schinke, J.M. Rueger, M. Amling, Biomaterials 25 (2004) 3963.
[38] E. Landi, A. Tampieri, G. Celotti, R. Langenati, M. Sandri, S. Sprio, Biomaterials 26 (2005) 2835.
[39] A.C. Tas, J. Eur. Ceram. Soc. 20 (2000) 2389.
[40] D. Bayraktar, A.C. Tas, J. Mater. Sci. Lett. 20 (2001) 401.
[41] N. Sasaki, S. Odajima, J. Biomech. 29 (1996) 655.
[42] L. Vitagliano, G. Nemethy, A. Zagari, H.A. Scheraga, J. Mol. Biol. 247 (1995) 69.
[43] S.H. Rhee, J. Tanaka, J. Am. Ceram. Soc. 81 (1998) 3029.
[44] D. Lickorish, J.A.M. Ramshaw, J.A. Werkmeister, V. Glattauer, C.R. Howlett, J. Biomed. Mater. Res. 68A (2004) 19.
[45] E.K. Girija, Y. Yokogawa, F. Nagata, Chem. Lett. 7 (2002) 702.
[46] A. Oyane, H.M. Kim, T. Furuya, T. Kokubo, T. Miyazaki, T. Nakamura, J. Biomed. Mater. Res. 65A (2003) 188.
[47] J.H. Bradt, M. Mertig, A. Teresiak, W. Pompe, Chem. Mater. 11 (1999) 2694.
[48] A. Yokoyama, M. Gelinsky, T. Kawasaki, T. Kohgo, U. Koenig, W. Pompe, F. Watari, J. Biomed. Mater. Res. 75B (2005) 464.
[49] L. Yubao, K. DeGroot, J. DeWijn, C.P.A.T. Klein, S.V.D. Meer, J. Mater. Sci., Mater. Med. 5 (1994) 326.
[50] M. Yoshimura, H. Suda, K. Okamoto, K. Ioku, J. Mater. Sci. 29 (1994) 3399.
[51] T. Iizuka, A. Nozuma, J. Ceram. Soc. Jpn. 106 (1998) 820.
[52] A.C. Tas, J. Am. Ceram. Soc. 84 (2001) 295.
[53] A.C. Tas, Powder Diffr. 16 (2001) 102.
[54] H. Dreessmann, Beitr. Klin. Med. Chir. 9 (1892) 804.
[55] L.F. Peltier, Clin. Ortop. 21 (1961) 1.
[56] A.S. Coetzee, Arch. Otolaryngol 106 (1980) 405.
[57] M. Nilsson, L. Wielanek, J.S. Wang, K.E. Tanner, L. Lidgren, J. Mater. Sci., Mater. Med. 14 (2003) 399.
[58] Smith & Nephew, Inc., Memphis, TN, USA (http://ortho.smith-nephew.com/us/Standard.asp?NodeId=3287).
[59] Wright Medical Technology, Inc., Arlington, TN, USA (http://www.wmt.com/Physicians/Products/Biologics/OSTEOSETBoneGraftSubstitute.asp).
[60] Orthogen Corp., Springfield, NJ, USA (http://www.orthogencorp.com/pages/886726/index.htm).
[61] Lifecore Biomedical, Inc., Chaska, MN, USA (http://www.lifecore.com/products/capset.asp).
[62] G.E. Pecora, D. De Leonardis, C. Della-Rocca, R. Cornelini, C. Cortesini, Int. J. Oral Maxillofac. Implants 13 (1998) 866.
[63] C.M. Kelly, R.M. Wilkins, G. Gitelis, C. Hartjen, J.T. Watson, P.T. Kim, Clin. Ortop. 382 (2001) 42.
[64] B.K. Tay, V.V. Patel, D.S. Bradford, Orthop. Clin. North Am. 30 (1999) 615.
[65] F. Carinci, A. Piattelli, G. Stabellini, A. Palmieri, L. Scapoli, G. Laino, S. Caputi, F. Pezzetti, J. Biomed. Mater. Res. 71B (2004) 260.
[66] A. Strauss, Lokaler Antibiotikumtraeger aus Kalziumsulfat: Vertraeglichkeit im Gewebe und Pharmakokinetik der angewendeten Antibiotika nach Implantation in Kaninchen. Biomaterialien in der Medizin, Koehler, Giessen, Germany, 1999, p. 105.
[67] C. Liang, Z. Li, D. Yang, Y. Li, Z. Yang, W.W. Lu, Mater. Chem. Phys. 88 (2004) 285.
[68] M. Bohner, Biomaterials 25 (2004) 741.
[69] M. Nilsson, E. Fernandez, S. Sarda, L. Lidgren, J.A. Planell, J. Biomed. Mater. Res. 61 (2002) 600.
[70] R.I. Martin, P.W. Brown, J. Cryst. Growth 183 (1998) 417.
[71] E.M. Ooms, J.G.C. Wolke, J.P.C.M. van der Waerden, J.A. Jansen, J. Biomed. Mater. Res. 66B (2003) 447.
[72] N.B. Singh, J. Am. Ceram. Soc. 88 (2005) 196.
[73] H.U. Hummel, B. Abdussaljamow, H.B. Fischer, J. Stark, ZKG Int. 54 (2001) 458.

[74] L. Tortet, J.R. Gavarri, G. Nihoul, A.J. Dianoux, J. Solid State Chem. 132 (1997) 6.
[75] A. Lebugle, B. Sallek, A. Tai-Tai, J. Mater. Chem. 9 (1999) 2511.
[76] H. McDowell, W.E. Brown, J.R. Sutter, Inorg. Chem. 10 (1971) 1638.
[77] F.C.M. Driessens, R.M.H. Verbeeck, Biominerals, CRC Press, Boca Raton, FL, 1990, p. 37.
[78] A.G. de la Torre, M.G. Lopez-Olmo, C. Alvarez-Rua, S. Garcia-Granda, M.A.G. Aranda, Powder Diffr. 19 (2004) 240.
[79] A. Hina, G.H. Nancollas, M. Grynpas, J. Cryst. Growth 223 (2001) 213.
[80] B.S. Krumgalz, A. Starinsky, K.S. Pitzer, J. Solid Chem. 28 (1999) 667.
[81] E.D. Spoerke, S.I. Stupp, Biomaterials 26 (2005) 5120.
[82] Y. Ling, G.P. Demopoulos, Ind. Eng. Chem. Res. 44 (2005) 715.
[83] J. Carlson, M. Nilsson, E. Fernandez, J.A. Planell, Biomaterials 24 (2003) 71.
[84] M.A. Rauschmann, T.A. Wichelhaus, V. Stirnal, E. Dingeldein, L. Zichner, R. Schnettler, V. Alt, Biomaterials 26 (2005) 2677.
[85] E. Fernandez, M.D. Vlada, M.M. Gela, J. Lopez, R. Torres, J.V. Cauich, M. Bohner, Biomaterials 26 (2005) 3395.
[86] C. Niedhart, U. Maus, W. Piroth, O. Miltner, B. Schmidt-Rohlfing, C.H. Siebert, J. Biomed. Mater. Res. 71B (2004) 123.
[87] Y. Murashima, G. Yoshikawa, R. Wadachi, N. Sawada, H. Suda, Int. Endod. J. 35 (2002) 768.
[88] S. Joschek, B. Nies, R. Krotz, A. Gopferich, Biomaterials 21 (2000) 1645.
[89] E.M. Ooms, J.G.C. Wolke, J.P.C.M. van der Waerden, J.A. Jansen, J. Biomed. Mater. Res. 61 (2002) 9.